Eur. Phys. J. D **40**, 317–323 (2006)
DOI: 10.1140/epjd/e2006-00172-5

THE EUROPEAN PHYSICAL JOURNAL D

Theoretical study of the $5p^5 6s - 5p^6$ spectra of neutral xenon

C.Z. Dong[1,a], S. Fritzsche[2], and B. Fricke[2]

[1] Department of Physics, Northwest Normal University, Lanzhou 730070, P.R. China
[2] Institut für Physik, Universität Kassel, 34132 Kassel, Germany

Received 14 October 2005 / Received in final form 4 April 2006
Published online 18 July 2006 – © EDP Sciences, Società Italiana di Fisica, Springer-Verlag 2006

Abstract. Recent high precision measurements on the lifetime of the metastable $6s[3/2]_2$ state of atomic xenon display a difference with previous predictions by a factor of 2–3. In the present work, a systematic relaxation and correlation approach, which has been developed on the basis of a widely used multi-configuration Dirac-Fock method, is applied to study the electric dipole allowed E1 and forbidden M1, E2 and M2 transitions between the $5p^5 6s$ and $5p^6$ configurations. We systematically include the correlation effects which arise from all the single and double excitations from the occupied $\{5s, 5p\}$ shells into the $\{ns, np, (n-1)d\}$ ($n = 6$–10) active sets and the relaxation effects caused by change of the electron density between the radiative initial- and final-states. This study not only reduces greatly the existing discrepancy in the lifetime of the $6s[3/2]_2$ state, but also presents rather consistent results for both the lifetime of the metastable $6s'[1/2]_0$ state and the oscillator strength of the $5p^5 6s - 5p^6$ E1 resonant transitions.

PACS. 32.70.Cs Oscillator strengths, lifetimes, transition moments

1 Introduction

The ground state of xenon is formed by the very stable closed-shell configuration $5p^6$. The first four excited states are formed by the configuration $5p^5 6s$. These excited levels are separated into two pairs by their parent terms $5p^5(^2\mathrm{P}_{3/2})$ and $5p^5(^2\mathrm{P}_{1/2})$, respectively, and are designated as $6s[3/2]_2$ and $6s[3/2]_1$ as well as $6s'[1/2]_1$ and $6s'[1/2]_0$ in the standard Jl coupling scheme [1]. The lowest excited state $6s[3/2]_2$ can decay only via a magnetic quadrupole (M2) radiation into the ground state $5p^6\ {}^1\mathrm{S}_0$. The $6s'[1/2]_0$ state can decay to either the $6s[3/2]_1$ by a magnetic dipole (M1) transition or to the $6s[3/2]_2$ by an electric quadrupole (E2) radiation. The $6s[3/2]_1$ and $6s'[1/2]_1$ states can decay to the $5p^6\ {}^1\mathrm{S}_0$ ground state via an electric dipole (E1) transition.

Recently, a high precision measurement performed in a magnetic optic trap (MOT) by Walhout et al. [2] gave a lifetime of 42.9 ± 3.9 s for the $6s[3/2]_2$ metastable state of atomic xenon. However, the experimental lifetime differs from the previous prediction of 150 s of Small-Warren et al. [3] by about a factor of 3. In order to explain this big discrepancy, Indelicato et al. [4] also calculated the lifetime using a multi-configuration Dirac-Fock (MCDF) method. However, their theoretical result of 96 s is still twice the experimental value of 42.9 s. Later the lifetime of the $6s'[1/2]_0$ state was also measured as $0.128^{+0.122}_{-0.042}$ s by the same group of Walhout et al. [5]. But there was a very big uncertainty in the observation. In 2001, Mishra and Balasubramanian [6] also calculated the lifetimes of the $6s[3/2]_2$ and $6s'[1/2]_0$ states by including a hyperfine quenching effect. It was found that the hyperfine quenching effect results in a remarkable reduction of lifetimes of the $6s[3/2]_2$ and $6s'[1/2]_0$ states for the isotopic atomic xenon with odd nuclear spin, but such an effect is absent for the atomic xenon with even nuclear spin. In the latter case, their theoretical lifetime of 100 s for the $6s[3/2]_2$ state was still over twice the existing experimental value [5].

The oscillator strength of the $5p^5 6s - 5p^6$ E1 transition has also been a challenge in both theory and experiment. Although there have been many calculations and measurements [7–32], some remarkable discrepancies still exist among the different theories and experiments as well as the theories and experiments themselves. For instance, the relativistic many-body calculation of Euripides et al. [7] gave excellent agreement with several recent measurements by Molino et al. [14], Anderson et al. [15] and Chan et al. [16] for the strongest $6s[3/2]_1 - 5p^6\ {}^1\mathrm{S}_0$ transition. However for another line, i.e. the $6s'[1/2]_1 - 5p^6\ {}^1\mathrm{S}_0$ transition, they did not provide any available new result.

From a theoretical point of view, the difficulty in treating these spectra may arise from the following three points: (i) due to a large splitting between the two parent terms $5p^5(^2\mathrm{P}_{1/2})$ and $5p^5(^2\mathrm{P}_{3/2})$, the LS coupling

[a] e-mail: dongcz@nwnu.edu.cn

condition is broken completely in all the excited states. As a result, the $5p^5(^2P_{3/2})5d$ levels lie very close to the $5p^5(^2P_{1/2})6s$. This leads to strong configuration interaction among these levels; (ii) the probability of a radiation transition involving a final state with a stable closed-shell $5p^6$ and an initial state with two open sub-shells, might be influenced seriously by the obvious differences between the initial and final orbital sets; (iii) relativistic effect and quantum electrodynamic (QED) effects should also be very important in such a heavy atom. In order to acquire satisfactory theoretical results for these spectra, systematic consideration of all of these effects is necessary.

Recently, on the basis of the widely used MCDF method [33] a new computational procedure which can treat relaxation and correlation effects systematically has been developed by us [34,35]. Using this procedure, we have successfully studied several complex atomic systems with open p and d shells [36–38]. In this present work, the same method is further used to study the electric dipole allowed E1 and forbidden M1, E2 and M2 transitions between the $5p^56s$ and $5p^6$ configurations of xenon. In Section 2, a short description of the theoretical method and computational procedure is given. The calculated lifetimes and oscillator strengths as well as some possible comparisons with different experiments and calculations are presented in Section 3. Finally, a brief summary is given in Section 4.

2 Theoretical method and computational procedures

The multiconfiguration Dirac-Fock (MCDF) method and the corresponding programs which are used for calculating the wavefunctions and transition probabilities have been described in detail [33–35]. Therefore, we will only give a brief account here of the MCDF model and the treatment of relaxation and correlation effects for many–electron atoms.

2.1 Calculation of energies and transition probabilities

In the MCDF method, the atomic state wavefunctions are taken as a linear combination of CSF of the same total angular momentum J and parity P,

$$|\psi_\alpha(PJM)\rangle = \sum_{r=1}^{n_c} c_r(\alpha)|\gamma_r PJM\rangle, \qquad (1)$$

where n_c is the number of CSF and $c_r(\alpha)$ are the mixing coefficients in that basis. For all practical computations, the (proper) choice of the many–electron CSF basis finally determines to which extent electron–electron correlations are taken into account. A systematically enlarged basis of such a CSF is often used to distinguish between different *computational models* within the MCDF framework [33–35].

The energies of the atomic levels with symmetry J^P are obtained by diagonalizing the Dirac–Coulomb Hamiltonian matrix in the given basis. Further relativistic corrections to the level structure can be considered by utilizing the Dirac–Coulomb–Breit matrix or by adding some suitable (one–electron) estimates from QED. Breit interaction, which is the Coulomb interaction between two electrons due to exchange of a single transverse photon, is treated in the low-frequency limit ($\omega_{ij} \to 0$) as a perturbation, which can correct for the total energy and configuration mixing coefficient, but can not correct for the radial wavefunctions because it is not included in the self-consistent process. In addition, the most important quantum electrodynamic (QED) effects, i.e. the self-energy and the vacuum polarization, have also been included in the calculation of the energies as done in [35–38].

The transition probability for a radiative decay from initial state i to final state f can be calculated by

$$A_{fi} = \frac{2\pi}{2j_i+1} \sum_{M_i,M_f} \sum_{L} |M_{fi}^{(L)}|^2, \qquad (2)$$

where one has to average over the initial states of level i and sum over the final states of f. An additional summation runs, in principle, over all the *multipole* components L of the electro–magnetic field but, since higher–order components of the field are strongly suppressed, only the lowest order $L_{\min}$, which is allowed, need usually to be taken into account. The transition matrix elements

$$\begin{aligned} M_{fi}^{(L)} &= \langle\psi_f(P_f J_f M_f)|O^{(L)}|\psi_i(P_i J_i M_i)\rangle \\ &= \sum_{r,s} c_r(f)c_s(i)\langle\gamma_r P_f J_f M_f|O^{(L)}|\gamma_s P_i J_i M_i\rangle \end{aligned} \qquad (3)$$

are reduced according to the transition matrix within the CSF basis. Different computational procedures have been developed to calculate this matrix for symmetry–adapted functions which are built from two incomplete orthogonal orbital sets. In our programs, the matrix elements are further represented in terms of Slater determinants as well as Löwdin's expressions [40]

$$\begin{aligned} &\langle\gamma_r P_f J_f M_f|O^{(L)}|\gamma_s P_i J_i M_i\rangle = \\ &\qquad \sum_{p,q}\sum_{k,l} B_{rp}B_{sq}\langle\varphi_k|O^{(L)}|\varphi_l\rangle D_{pq}(kl). \end{aligned} \qquad (4)$$

In this representation, $D_{pq}(kl) = \det\{d_{pq}(kl)\}$ denotes the determinant of the (one–electron) *overlap* matrix elements $d_{kl} = \langle\varphi_k|\varphi_l\rangle$ from which the pth raw and qth column has been deleted. The one–particle matrix elements for the interaction with the radiation field

$$\begin{aligned} \langle\varphi_k|O^{(L)}|\varphi_l\rangle = &\left(\frac{(2j_l+1)\,\omega}{\pi c}\right)^{1/2} \\ &\times (-1)^{j_l-1/2}\begin{pmatrix} j_k & L & j_l \\ \frac{1}{2} & 0 & -\frac{1}{2}\end{pmatrix}\overline{M}_{kl} \end{aligned} \qquad (5)$$

can be reduced further by the Wigner–Eckart theorem and written in terms of the radial integrals $\overline{M}_{kl}$ which need to

be distinguished for the different multipoles (E1, M1, E2, ...) and gauges of the radiation field. Usually two different gauges, namely the Babushkin and Coulomb gauge are considered which, in the non–relativistic limit, correspond to the length and velocity gauges. They may help obtain insight into the accuracy of the calculation, although the gauge invariance of the results is itself a *necessary but not sufficient condition* to draw conclusions about the (physical) convergence of the results. An efficient program for the computation of *relaxed–orbital* transition probabilities has been developed recently by us within the framework of the RATIP package [34,35] which now supports wavefunction expansion of several hundred thousand determinants even using standard PCs.

2.2 Consideration of relaxation and correlation effects

The relaxation of the electron density refers to the change of the bound-state electron orbits due to the emission or absorption of a photon. To include this effect in the wave functions of the initial and final states in a straightforward manner, a separated MCDF calculation is necessary for the atomic levels of interest. Such an independent computation of the wave functions, however, yields two sets of electron orbits which are not quite orthogonal to each other. To incorporate the effects of relaxation in the computation of transition amplitudes, the *overlap* of the initial- and final-state orbits has to be treated properly in the evaluation of the many-electron matrix elements as outlined in the previous subsection. Of course, this evaluation is also relative to how the computations ought to be organized: they are often only feasible, if the levels are arranged in several groups according to their symmetry, i.e. their total angular momenta and parities. In the present study, we divided the levels into four groups: one for the $5p^6\ ^1\mathrm{S}_0$ ground state, one for the two $J = 0$ excited states of the $5p^5 6s + 5p^5 5d$, one for the four $J = 1$ levels of the $5p^5 6s + 5p^5 5d$ and one for the $J = 2$ level of the $5p^5 6s$. For these groups, separate computations were carried out through all the steps in our series of approximations (see below), using the (extended) optimal level model of the GRASP92 package [33]. To display, for instance, the influence of the relaxation effects on the spectroscopically occupied orbits, Table 1 shows the *mean orbital radius* $\langle r \rangle$ of the outmost $5s$ and $5p$ orbits corresponding to the $5s^2 5p^6\ ^1\mathrm{S}_0$ ground state and the $J = 1$ excited states. As seen from Table 1, the mean orbital radii in the excited levels with $J = 1$ are always smaller, when compared with the orbits in the ground state. For the $5p_{1/2}$ and $5p_{3/2}$ orbits, the differences are in the range of 5%, compared to the corresponding ground–state orbits. Thus, it is obvious that these relaxation effects in the electron density cannot be neglected, in particular, if the decay probabilities are considered for weak lines.

In order to consider the influence of electron–electron correlation, a series of steps have been carried out for the four level groups defined above, using an active space method. In this method, one starts from one or a few reference configurations chosen on the basis of the spectroscopic occupied orbits. Then, the list of CSF of a given symmetry is generated by exciting electrons from these reference configurations within an active set of orbits. In the present study, the configurations $5p^6$ and $5p^5 6s + 5p^5 5d$ are used as references, for the even and odd parity states respectively. All the possible single (S) and double (D) excitations from the $\{5s,\ 5p\}$ occupied shells up to the active sets $\{ns, np, (n-1)d\}$ $(n = 6\text{–}10)$ are considered. The number of CSF used in the ASF expansions for the different level groups is listed in Table 2. Due to the fact that the number of the CSF grows so rapidly with increase of the size of the active sets, we are not able to include the excitations with n larger than 10 and l larger than 3 in the present active sets. But as we will see in Section 3, this approximation can explain most important correlation effects for the present considered states and provide an excellent convergence result.

Table 1. Mean orbital radii (in atomic unit) of the occupied orbits $5s$ and $5p$ in the $^1\mathrm{S}_0$ ground state and the $6s'[1/2]_1$ and $6s[3/2]_1$ excited states in Xe I.

	Ground state	Excited states
Orbits	$5p^6\ ^1\mathrm{S}_0$	$6s'[1/2]_1 + 6s[3/2]_1$
$5s$	1.9011	1.8557
$5p_{1/2}$	2.2382	2.1475
$5p_{3/2}$	2.3479	2.2389

3 Results and discussions

Using the computational procedure from above, the electric dipole allowed E1 and forbidden M1, E2 and M2 transitions between the $5p^5 6s$ and $5p^6$ configurations of xenon are calculated and analyzed systematically. Below, we present and discuss the lifetimes of the metastable $6s[3/2]_2$ and $6s'[1/2]_0$ levels as well as the oscillator strengths of the $6s[3/2]_1 - 5p^6\ ^1\mathrm{S}_0$ and $6s'[1/2]_1 - 5p^6\ ^1\mathrm{S}_0$ transitions.

3.1 Lifetime of the metastable state 6s[3/2]$_2$

The lowest-excited $6s[3/2]_2$ level can only decay into the ground state $5p^6\ ^1\mathrm{S}_0$ through a M2 transition. Since this magnetic quadruple line is a very weak transition [2–4,6], the influence of relaxation and correlation is expected to be very important. In this subsection, the different correlation contributions to the binding energy and main components of the wavefunction expansions of the initial and final states are studied systematically. By increasing the size of the active sets, the convergence of the lifetime of the $6s[3/2]_2$ state is analyzed for the two cases with and without relaxation effects. Finally, the lifetime of the $6s[3/2]_2$ state is presented by applying an active set with $n \leq 10$.

Figure 1 displays the relative contribution of the correlation effects on the independence of the $5p^6\ ^1\mathrm{S}_0$ and $6s[3/2]_2$ level energies on the size of the active space. In this figure, the relative correlation contribution refers to

Table 2. Number of the CSF in the expansion of ASF and number of the levels as used in the optimization of the wavefunctions of different symmetry. For the active sets with $n \geq 9$, only the $5p^5 6s$ reference configuration has been used in the generation of the CSF lists.

			Number of CSF in $\{ns, np, (n-1)d\}$				
Configurations	J	Number of level	6	7	8	9	10
$5p^6$	0	1	53	238	403	701	1081
$5p^5 6s + 5p^5 5d$	0	2	301	1690	4243	5428	6961
	1	4	781	4424	11126	14128	18010
	2	1	963	5562	14059	17579	22131

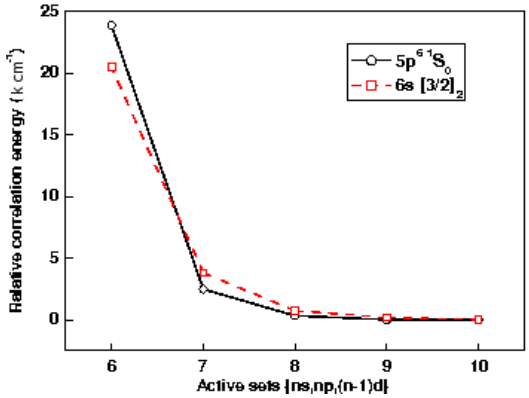

Fig. 1. Relative correlation energies of the $5p^6\ ^1\mathrm{S}_0$ and $6s[3/2]_2$ levels as a function of active set as used in the calculations. The relative correlation energy refers to the energy difference between the results of active sets n_0 and $n_0 - 1$.

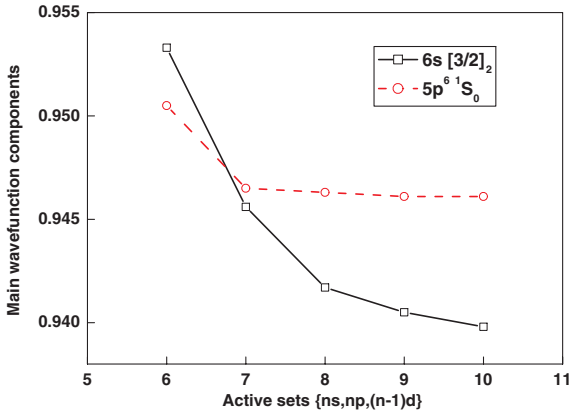

Fig. 2. Main components of the $5p^6\ ^1\mathrm{S}_0$ and $6s[3/2]_2$ levels as a function of the active set as used in the calculations.

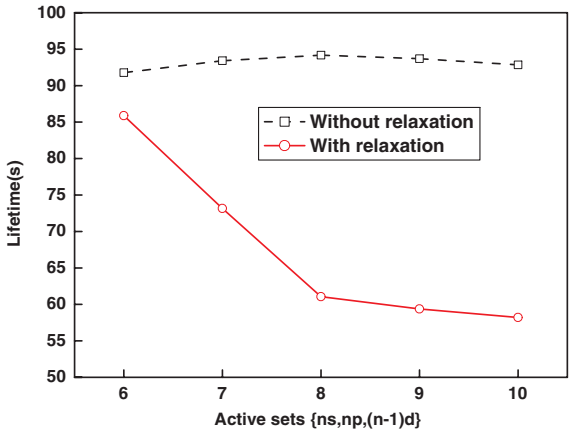

Fig. 3. Effects of relaxation and correlation on the lifetime of the metastable $6s[3/2]_2$ level in Xe I.

the difference of the binding energies as obtained from the active sets with $n \leq n_0$ and $n_0 - 1$. As seen from Figure 1, the incorporation of excitations with $n \leq 6...8$ play a very important role for the level energies for both, the $5p^6\ ^1\mathrm{S}_0$ and $6s[3/2]_2$ states. By increasing the size of the active sets, the convergence is faster for the ground state $5p^6\ ^1\mathrm{S}_0$ than that of the excited state $6s[3/2]_2$. By applying an active set with $n \leq 10$, we obtain an error with an accuracy of 0.9% for the excitation energy.

Besides the binding energy, the wavefunction expansion coefficient is another quantity which is directly associated with the correlation effect. It is found that in the present calculations, there is only one dominant component for both the radiative initial state $6s[3/2]_2$ and final state $5p^6\ ^1\mathrm{S}_0$, while the other components are rather small (usually less than 0.009). In Figure 2, we further show the convergence behaviour of the main components corresponding to the two states $6s[3/2]_2$ and $5p^6\ ^1\mathrm{S}_0$, respectively. As seen from Figure 2, the influences from the active sets having higher n are more important for the excited state $6s[3/2]_2$ than for the ground state $5p^6\ ^1\mathrm{S}_0$. This is in accordance with the convergence behaviour of the correlation energy as mentioned above.

In Figure 3, the change of the theoretical lifetime as a function of the size of the active sets in the cases with and without relaxation effects is shown. As seen from Figure 3, in the case where the relaxation effect is included, the theoretical lifetime becomes rapidly small with increasing size of the active sets, especially in the lower active sets $n = 6$–8. As expected, the contributions from the active sets $n \geq 9$ are small, only reduce the lifetime by 2.86 s. However, in the case without relaxation, namely neglecting all overlaps by assuming orthogonality among the wavefunctions with the same symmetry, the theoretical lifetime changes only very little with increasing size of the active sets. Figure 3 reveals clearly the importance of considering relaxation and correlation effects in an unified way in a systematic calculation of transition probability. In fact, the inclusion of relaxation effects can dramatically improve the calculation of transition probabilities. It also has the further advantage that one is not required to apply

Table 3. Theoretical and experimental excitation energies and lifetimes of the $6s[3/2]_2$ level in Xe I.

Method and author		Energy (cm^{-1})	Lifetime (s)
Theory	This work	67644	58.2
	Mishra et al. [6]		100
	Indelicato et al. [4]		96
	Small-Warren et al. [3]		150
Experiment	Walhout et al. [2]	67068	42.9 ± 3.9

Table 4. Theoretical and experimental excitation energies and lifetimes of the $6s'[1/2]_0$ level in Xe I.

Method and author		Energy (cm^{-1})	Lifetime (s)
Theory	This work	76682	0.111
	Mishra et al. [6]		0.084
	Small-Warren et al. [3]		0.078
Experiment	Walhout et al. [5]	76197	$0.128^{+0.122}_{-0.042}$

such large wavefunction expansions in order to achieve a given accuracy.

In Table 3, the theoretical lifetime of the $6s[3/2]_2$ state is presented in the active set $n = 10$. For comparison, the available measurement and previous predictions are also given. As seen from Table 3, the present calculation is quite close to the recent experiment [2] compared to the previous predictions [3,4,6].

We nonetheless have to mention that there is still a big disagreement of 36% between the present calculation and the experiment. From a theoretical point of view, the disagreement may arise from the following reasons: (i) although lots of important correlations have been included in the present calculation, there are still some correlations, such as the core-core correlations from the $4l$ sub-shells and the valence correlations from the more higher active sets n and l, which are not included here; (ii) the contributions from the Breit interaction and QED corrections are not included completely, they are treated only as perturbations in the present calculations for energies.

3.2 Lifetime of the metastable state $6s'[1/2]_0$

The $6s'[1/2]_0$ metastable state can decay to the excited state $6s[3/2]_1$ by a M1 transition, also to the $6s[3/2]_2$ by a E2 transition. But due to the contribution from the M1 transition, this contribution is far larger than that of the E2 transition. Therefore the lifetime of the metastable state $6s'[1/2]_0$ is determined mainly by the M1 decay. In Table 4, the calculated lifetime of the $6s'[1/2]_0$ state is listed. For comparison, the available measurement and previous calculations are also given.

As seen from Table 4, the present calculated lifetime of the $6s'[1/2]_0$ state is in good agreement with the experimental spontaneous emission lifetime [5], but it is longer by 30% compared to the previous predictions [3,6]. The total experimental lifetime of this level is not only given by the spontaneous emission from the $6s'[1/2]_0 - 6s[3/2]_1$ M1 transition, but also depends on a blackbody-induced deexcitation to the $6p[1/2]_1$ state as indicated in reference [5]. Therefore the experimental uncertainty is too big for a more accurate comparison with the present calculation.

A detailed study on the influence of correlation effects with respect to the lifetime is also carried out. It is found that the theoretical lifetime is changed by only 0.6% by inclusion of the active sets from $n = 6$ to $n = 8$. Therefore, the contributions from the higher active sets $n = 9$ and $n = 10$ should be very small, and are not considered in the final calculation.

In addition, it is worth pointing out that a direct consideration of the configuration interaction between the $6s'[1/2]_0$ and $5d[3/2]_0$ levels is very important. The experimental energies of these two levels are 76197 cm^{-1} and 79772 cm^{-1}, respectively. They lie very close to each other. As found in the calculation, the mixing coefficient between these two levels reaches about 0.23 in the active set $n = 8$. This mixture results in a great enlargement of the theoretical lifetime. For example, in the case only including the $6s'[1/2]_0$ level in the calculation, the theoretical lifetime is only 0.086 s in the active set $n = 8$. When we treat those two levels together, the theoretical lifetime becomes 0.111 s in the same active set.

3.3 Oscillator strengths of the $5p^5$ 6s – $5p^6$ E1 transition

The electric dipole allowed $5p^5 6s - 5p^6$ transition produces two separate single lines $6s[3/2]_1 - 5p^6\ {}^1S_0$ and $6s'[1/2]_1 - 5p^6\ {}^1S_0$.

In order to present the results as accurately as possible, a further study on the convergence of the oscillator strengths (or transition probabilities) of these two lines has also been carried out. It is found that the oscillator strengths are not too sensitive to the correlations. As a result, the calculated oscillator strengths change very little with the systematic increase of the size of the active sets. For example, the calculated result for the $6s[3/2]_1 - 5p^6\ {}^1S_0$ line is 0.303/0.303 (refers to the ratio of the results in length and velocity gauges) in the active set $n = 6$, and only reduces to 0.267/0.263 in the active set

Table 5. Comparison of the theoretical and experimental oscillator strengths of the $5p^5 6s - 5p^6$ E1 transitions in Xe I. gf_L and gf_V refer to the oscillator strengths in length and velocity gauges, respectively.

Method and author		$6s[3/2]_1 - 5p^6\ {}^1\mathrm{S}_0$ gf_L/gf_V	$6s'[1/2]_1 - 5p^6\ {}^1\mathrm{S}_0$ gf_L/gf_V
Theory	This work	0.271/0.263	0.158/0.154
	Euripides et al. [7]	0.249/0.256	
	Aymar et al. [8]	0.282/0.294	0.306/0.270
	Geiger [9]	0.28	0.365
	Aymar et al. [10]	0.273/0.177	0.235/0.118
	Kim et al. [11]	0.212	0.189
	Gruzdev [12]	0.28	0.25
	Dowand Knox[13]	0.194	0.147
Experiment	Molino Garcia et al. [14]	0.260 ± 0.010	0.170 ± 0.007
	Anderson et al. [15]	0.264 ± 0.016	
	Chan et al. [16]	0.273 ± 0.014	0.186 ± 0.009
	Suzuki et al. [17]	0.222 ± 0.027	0.158 ± 0.019
	Ferrell et al. [18]	0.260 ± 0.05	0.19 ± 0.04
	Salamero et al. [19]	0.226 ± 0.026	
	Bideau-Mehu et al. [20]	0.268 ± 0.008	
	Smith et al. [21]	0.244 ± 0.015	
	Wieme et al. [22]	0.226 ± 0.025	
	Matthias et al. [23]	0.263 ± 0.007	0.229 ± 0.007
	Delage et al. [24]	0.183 ± 0.073	0.169 ± 0.068
	Wieme et al. [25]	0.213 ± 0.020	0.180 ± 0.040
	Geiger [26]	0.26 ± 0.05	0.19 ± 0.03
	Wilkinson [27]	0.260 ± 0.020	0.270 ± 0.020
	Chashchina et al. [28]	0.28 ± 0.05	
	Anderson [29]	0.256 ± 0.008	0.238 ± 0.015
Semi-empirical simulation	Chen et al. [30]	0.202 ± 0.030	0.147 ± 0.022
	Haffad et al. [31]	0.215 ± 0.010	0.173 ± 0.033
	Bessis et al. [32]	0.208 ± 0.027	0.141 ± 0.019

$n = 8$. Furthermore, the contributions from the higher active sets with $n \geq 9$ are even smaller, and are not included in the present calculations.

In Table 5, the calculated oscillator strengths and transition probabilities are listed in the active set $n = 8$. For comparison, the previous calculations [7–13], experiments [14–29], and several semi-empirical simulations [30–32] are also shown in Table 5.

As seen from Table 5, for the $6s[3/2]_1 - 5p^6\ {}^1\mathrm{S}_0$ line, the present calculation is in very good agreement with the newest relativistic many-body calculation of Euripides et al. [7] and most of the experimental data [14–16,18,20,21,26–29]; In the case of the $6s'[1/2]_1 - 5p^6\ {}^1\mathrm{S}_0$ line, the present result is also rather close to the calculation of Dow and Knox [13] and the experiments [14,16–18,24–26] as well as the extrapolated results of the general oscillator strengths (GOS) [30–32].

4 Conclusions

In summary, the electric dipole allowed E1 and forbidden M1, E2 and M2 transitions between the $5p^5 6s$ and $5p^6$ configurations have been studied systematically using a large scale MCDF method. With this investigation, we not only reduce greatly the existing discrepancy in the lifetime of the metastable $6s[3/2]_2$ state but also present rather consistent results for both the lifetime of the metastable $6s'[1/2]_0$ state and the oscillator strengths of the $5p^5 6s - 5p^6$ E1 resonant transitions.

From the present study, several important conclusions can be drawn which will be helpful also for the analysis of other complex atomic systems: (i) the two reference configurations $5p^5 6s + 5p^5 5d$ play an important role for improving the convergence of the present calculation as used successfully by O'Malley and Beck et al. [42,43] in calculating the lifetimes of xenon–like Cs and La; (ii) the inclusion of at least two additional angular orbits and two higher excitation layers in constructing an active set is necessary in order to obtain a converged result as pointed out before in several previous studies [36–38]; (iii) the incorporation of both the correlation and relaxation effects is found to improve dramatically the transition probabilities, especially for the weak lines such as the $6s[3/2]_2 - 5p^6(^1\mathrm{S}_0)$ M2 transition in the present study. Therefore, a systematic inclusion of these effects is very important for the calculation of complex atomic systems.

Addendum

Before this paper will be printed, we learned of two more recent works for the lifetime of the metastable $6s[3/2]_2$ state of atomic xenon [44,45]. One of them connects the

experimental observation of Lefers et al. [44], and the other is the relativistic configuration interaction (RCI) calculation of Beck [45]. The newest experimental result is in quite good agreement with the previous observation of Walhout et al. [2]. The RCI calculation of Beck [45] yields a result of 48.3 s by including the single and double excitations to the $\{ns, np, nd, nf, ng\}$ virtual orbits, which is also in good agreement with the two existing experiments. But a similar calculation by adding the $\{nf\}$ and $\{ng\}$ virtual orbits directly in our $\{ns, np, (n-1)d\}$ correlation models seems unable to yield such result. In order to explain the difference between the present calculation and that of Beck, some further calculations are currently underway.

This work has been supported by the National Natural Science Foundation of China (Grant Nos. 10376026, 10434100), the excellent Young Teachers Program of MOE, P.R. China, the Foundation of the Center of Theoretical Nuclear Physics, National Laboratory of Heavy Ion Accelerator of Lanzhou, and Kassel University.

References

1. C.E. Moore, *Atomic Energy Levels* (U.S. GPO, Washington D.C., 1971), Vol. II
2. M. Walhout, A. Witte, S.L. Rolston, Phys. Rev. Lett. **72**, 2843 (1994)
3. N.E. Small-Warren, L.-Y.C. Chiu, Phys. Rev. A **11**, 1777 (1975)
4. P. Indelicato et al., unpublished work (1994)
5. M. Walhout, U. Sterr, A. Witte, S.L. Rolston, Opt. Lett. **20**, 1192 (1995)
6. A.P. Mishra, T.K. Balasubramanian, J. Quant. Spectrosc. Radiat. Transf. **69**, 769 (2001)
7. E.N. Avgoustoglou, D.R. Beck, Phys. Rev. A **57**, 4286 (1998)
8. M. Aymar, M. Goulombe, At. Data Nucl. Data Tables **21**, 537 (1978)
9. J. Geiger, Z. Phys. A **282**, 129 (1977)
10. M. Aymar, S. Feneuille, M. Klapisch, Nucl. Instrum. Meth. **90**, 137 (1970)
11. Y.K. Kim, M. Inokuti, G.E. Chamberlain, S.R. Mielczarek, Phys. Rev. Lett. **21**, 1146 (1968)
12. P.F. Gruzdev, Opt. Spectrosc. **22**, 170 (1967)
13. J.D. Dow, R.S. Knox, Phys. Rev. **152**, 50 (1966)
14. J.C. Molino Garcia, W. Botticher, M. Kock, J. Quant. Spectrosc. Radiat. Transf. **55**, 169 (1996)
15. H.M. Anderson, S.D. Bergeson, D.A. Doughty, J.E. Lawler, Phys. Rev. A **51**, 211 (1995)
16. W.F. Chan, G. Cooper, X. Guo, G.R. Burton, C.E. Brion, Phys. Rev. A **46**, 149 (1992)
17. T.Y. Suzuki, Y. Sakai, B.S. Min, T. Takayanagi, K. Wakiya, H. Suzuki, T. Inaba, H. Takuma, Phys. Rev. A **43**, 5867 (1991)
18. W.R. Ferrell, M.G. Payne, W.R. Garrett, Phys. Rev. A **35**, 5020 (1987)
19. Y. Salamero, A. Birot, H. Brunet, J. Galy, P. Millet, J. Chem. Phys. **80**, 4774 (1984)
20. A. Bideau-Mehu, Y. Guern, R. Abjean, A. Johannin-Gilles, J. Quant. Spectrosc. Radiat. Transfer. **25**, 395 (1981)
21. P.L. Smith, G.G. Lombardi, B.L. Cardon, W.H. Parkinson, Appl. Opt. **20**, 647 (1981)
22. W. Wieme, M. Vanmarcke, Phys. Lett. **72A**, 215 (1979)
23. E. Matthias, R.A. Rosenberg, E.D. Poliakoff, M.G. White, S.T. Lee, D.A. Shirley, Chem. Phys. Lett. **52**, 239 (1977)
24. A. Delage, J.D. Carette, Phys. Rev. A **14**, 1345 (1976)
25. W. Wieme, P. Mortier, Physica **65**, 198 (1973)
26. J. Geiger, Phys. Lett. **33A**, 351 (1970)
27. P.G. Wilkinson, J. Quant. Spectrosc. Radiat. Transfer. **6**, 823 (1966)
28. G.I. Chashchina, E.Ya. Shreider, Opt. Spectrosc. **20**, 283 (1966)
29. D.K. Anderson, Phys. Rev. **137**, A21 (1965)
30. Z. Chen, A.Z. Msezane, J. Phys. B **31**, 1097 (1998)
31. A. Haffad, Z. Felfli, A.Z. Msezane, D. Bessis, Phys. Rev. Lett. **76**, 2456 (1996)
32. D. Bessis, A. Haffad, A.Z. Msezane, Phys. Rev. A **49**, 3366 (1994)
33. F.A. Parpia, C. Froese Fischer, I.P. Grant, Comput. Phys. Commun. **94**, 249 (1996)
34. S. Fritzsche, I.P. Grant, Comput. Phys. Commun. **103**, 277 (1997)
35. S. Fritzsche, C. Froese Fischer, Comput. Phys. Commun. **99**, 323 (1997); S. Fritzsche, C. Froese Fischer, C.Z. Dong, Comput. Phys. Commun. **124**, 340 (2000)
36. C.Z. Dong, S. Fritzsche, B. Fricke, W.-D. Sepp, Mon. Not. R. Astron. Soc. **307**, 809 (1999)
37. C.Z. Dong, S. Fritzsche, B. Fricke, W.-D. Sepp, J. Elec. Spec. Rel. Phen. **114–116**, 157 (2001)
38. C.Z. Dong, S. Fritzsche, B. Fricke, Eur. Phys. J. D **23**, 5 (2003)
39. B.O. Roos, P.R. Taylor, P.E.M. Siegbahn, Chem. Phys. **48**, 157 (1980)
40. P.O. Löwdin, Phys. Rev. **97**, 1474 (1955)
41. P. Indelicato, Phys. Rev. Lett. **77**, 3323 (1996)
42. S. M. O'Malley, D.R. Beck, Phys. Rev. A **54**, 3894 (1996)
43. D.R. Beck, Phys. Rev. A **57**, 4240 (1998)
44. J. Lefers, N. Miller, D. Rupke, D. Tong, M. Walhout, Phys. Rev. A **66**, 012507 (2002)
45. D.R. Beck, Phys. Rev. A **66**, 034502 (2002)